Hishe *et al. Environ Syst Res (2017) 6:26*
https://doi.org/10.1186/s40068-017-0103-8

Environmental Systems Research

RESEARCH Open Access

Effects of soil and water conservation on vegetation cover: a remote sensing based study in the Middle Suluh River Basin, northern Ethiopia

Solomon Hishe[1,2*], James Lyimo[2] and Woldeamlak Bewket[3]

Abstract

Background: Soil and water conservation (SWC) has been implemented in the Tigray Region of Ethiopia since 1985. Besides this, the agricultural development strategy of the region which was derived from the national agricultural development led industrialization strategy formulated in 1993 was focused on natural resources rehabilitation and conservations. Accordingly, each year a 20-days free labor work on SWC activities were contributed by the rural communities. Other programmes such as productive safety net programmes, and sustainable land management project were deploying their resources aiming to reverse the degraded landscape in the region.

Method: Multi-temporal remote sensing data of landsat imageries were used for estimating the normalized difference vegetation index, soil adjusted vegetation index (SAVI) and land surface temperature (LST) for the years 1985, 2000 and 2015. Long-term station based data on daily precipitation started from 1973 was aggregated to derive average annual precipitation (AAP) into three sections to correspond with the processed image data. The precipitation data then converted into raster format using the inverse distance weight interpolation method. The analysis was done using ENVI 5.3 software and results were mapped in ArcGIS 10.3 package. The correlation between AAP and SAVI; LST and SAVI was evaluated on village polygon based as well as pixel-by-pixel.

Results: The results based on village polygons show that there is statistical significant inverse relationship between SAVI and LST in all the study periods. The correlations between AAP and SAVI pixel-by-pixel were $r = -0.14$ in 2015 and $r = 0.06$, $r = 0.25$ for 2000 and 1985 respectively. In 1985, the total area with SAVI ≥ 0.2 was 23.57 km2. After 15 years (from 1985 to 2000), the total area with SAVI ≥ 0.2 increased to 64.94 km2. In 2015, the total area of SAVI with values ≥ 0.2 reached 67.11 km2, which is a 3.3% increment from year 2000.

Conclusion: Based on the field observation and the remote sensing analysis results, noticeable gain in vegetation cover improvement have been observed in the 30 years period. These improvements are attributable to the implementation of integrated SWC measures particularly in areas where exclosure areas were defined and protected by the local community. Therefore, this study concludes by providing a theoretical bases and an indicator data support for further research on vegetation restoration for the entire region.

Keywords: Soil adjusted vegetation index, Soil and water conservation, Landsat, Land surface temperature, Middle Suluh River Basin

Background

Geographic information system (GIS) and remote sensing (RS) have become fundamental tools for characterizing watersheds and landscapes. Remote sensing is one of the most widely used technologies for discerning effective

*Correspondence: solomonhw@yahoo.com
[1] Department of Geography and Environmental Studies, Mekelle University, P.O. Box 231, Mekelle, Ethiopia
Full list of author information is available at the end of the article

correlations of ecosystem properties via the reflectance of light in the spatial and spectral domain. Remote sensors, such as Landsat, SPOT, IKONOSs, MODIS and Quickbird, capture the reflectance from ground objects like vegetation which have their own unique spectral characteristics. The spectral signatures of photosynthetically and non-photosynthetically active vegetation show clear differences and are used to estimate the forage quantity and quality of grass prairie (Beeri et al. 2007) and vegetation density. Moderate to high resolution data are being extensively used at varying scales from local to regional landscapes for assessment of the ecosystem processes (Chawla et al. 2010).

In this investigation, the relationships between SAVI and LST; SAVI and long term AAP was assessed in the years 1985, 2000 and 2015 for the Middle Suluh River Basin in northern Ethiopia, thereby providing useful information about the effects of soil and water conservation on vegetation cover improvement.

The method of LST–NDVI space with standard meteorological data, as well as remote sensing data were combined by Moran et al. (1994), to estimate the water deficit index (WDI). However, the combination of SAVI and LST; NDVI and LST; SAVI and precipitation pixel-by-pixel bases can provide information about vegetation and moisture condition of the Earth surface. The major information used was the wavelengths of the thermal region, the visible/NIR region and station records of rainfall, which were assumed to be satisfactory for monitoring vegetation conditions.

Land degradation was a serious problem in the Tigray Region with severe denudation of vegetation cover, depletion of soil fertility, and deterioration of surface and ground water potential (Berhanu et al. 2003). In order to reduce the extent of such problems, substantial rehabilitation work has been done through SWC practices. Some studies claim that SWC practices in the Tigray Region were started between 1975–1991 during the Tigray People's Liberation Front (TPLF) movement with the effective mobilization of the rural communities (Carolyn and Kwadwo 2011). Another study by Esser et al. (2002) indicated that SWC was introduced with the assistance of donors, following the drought in Wello and Tigray in 1976. The agricultural development strategy of the region which was derived from the national Agricultural Development Led Industrialization (ADLI) strategy formulated in 1993 (Dercon and Zeitlin 2009) was focused on the rehabilitation, conservation and development of natural resources, and is known as a conservation-based agricultural development policy (Berhanu et al. 2003). As a policy emphasis, major strategies were designed in the region during the early 1990s for integrated soil and water conservation activities (Negusse et al. 2013). Environmental rehabilitation practices such as establishment and development of area exclosures and community woodlots; construction of check-dams; stone terraces; soil bunds; enforcement of rules and regulations for grazing areas; application of manure and compost were then implemented throughout the region (Berhanu et al. 2003; Carolyn and Kwadwo 2011).

Based on the socio-economic survey of 246 sample household heads (HH) in the study area, the average number of years a farmer practiced SWC was 23 years. The large proportion of the interviewed HHs (95.5%) reported that there was a declining in soil erosion and an improvement in vegetation cover over the past years. A study conducted by Nyssen et al. (2009) in the northern highlands of Tigray shows that it is possible to reverse environmental degradation through an active, farmer-centered SWC policy. Most of SWC focused studies conducted in northern Ethiopia looks at the effects to soil loss and run-off (Taye et al. 2013; Gebremichael et al. 2005; Selassie et al. 2015) and food security (Van der Veen and Tagel 2011). From this perspective, we can quantify the vegetation cover improvement attributed to from the effects of SWC by using GIS and RS application in a basin which is not previously studied.

Methods

Study area description

The Middle Suluh River Basin is located in the northern highland of Tigray Region, in Ethiopia. It covers a total area of 490 km^2, and with an altitude ranging from 1818 to 2744 m.a.s.l (Fig. 1). The study area consists of almost 28 lower administrative units, locally called "*Tabia*" which are situated in three districts, namely *Kilte_Awulaelo*, *Saesie Tsaeda Emba* and *Hawzen*. Out

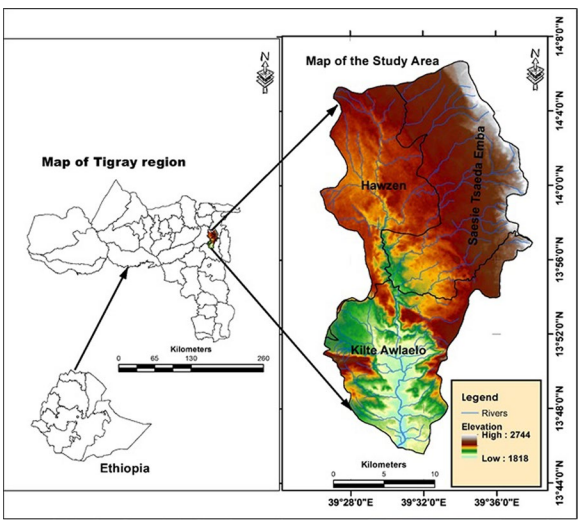

Fig. 1 Location and digital elevation model of Middle Suluh River Basin

of the 28 *tabias*, only 15 *tabias* have over 50% of their territory within the Middle Suluh River Basin. According to Bizuneh (2014) cited in HTSL (1976) and WAPCOS (2002), the Suluh Basin is mainly characterized by Precambrian basement rocks, Paleozoic, Mesozoic rocks and Younger tertiary and Quaternary deposits, with lithological units at the Precambrian basement, Enticho sandstone, Tillite, Adigrat sandstone, Transition, Mesozoic limestone, and Quaternary alluvial sediments. The major economic activity of the area is crop and livestock production. The Suluh River flows from north to south dissecting the study area into two halves. Since the study area is dominated with sandstone, many youths were engaged in extracting sand from the river bed to generate income by selling them for construction purposes. Such activity is practiced after the month of August when the rainy season starts to end and run-off gradually deposits the sand on the river bed.

The study area is dominated by five soil types, namely *Leptosol* (37.6%), *Luvisol* (22.6%), *Cambisol* (22.8%), *Regosol* (14.7%) and *Fluvisol* (2.3%). The economy of the households was based on agricultural production, and is mainly dependent on rainfed agriculture. Some household's practice small scale surface irrigation via micro dams and hand dug well water sources. According to FAO (2006) slope classification, 60% of the topography within the basin is flat to gently sloping and the remaining 40% from strongly sloping to very steep. Based on altitude, temperature and precipitation parameters, the agro-ecology of the area is described as warm temperate (*Woina dega*) zone (58%); and temperate (*Dega*) zone (42%). The mean annual rainfall from three stations around the study area for the period 2006–2015 was 536 mm with uneven distribution and the mean annual temperature is 18.7 °C.

Table 1 Landsat data used in the analysis and their specification

Satellite (sensor)	Path/row	Acquisition date	Spatial resolution (m)
Landsat 5-TM	169/50	26 February 1985	30
Landsat TM-5	169/50	15 March 2000	30
Landsat 8 (OLI)	169/50	13 February 2015	30

Normalized difference vegetation index

Many vegetation indices have been developed to assess vegetation conditions. Among them, the normalized difference vegetation index (NDVI), which was proposed by Rouse et al. (1973), is a numerical indicator that uses the visible and near-infrared bands of the electromagnetic

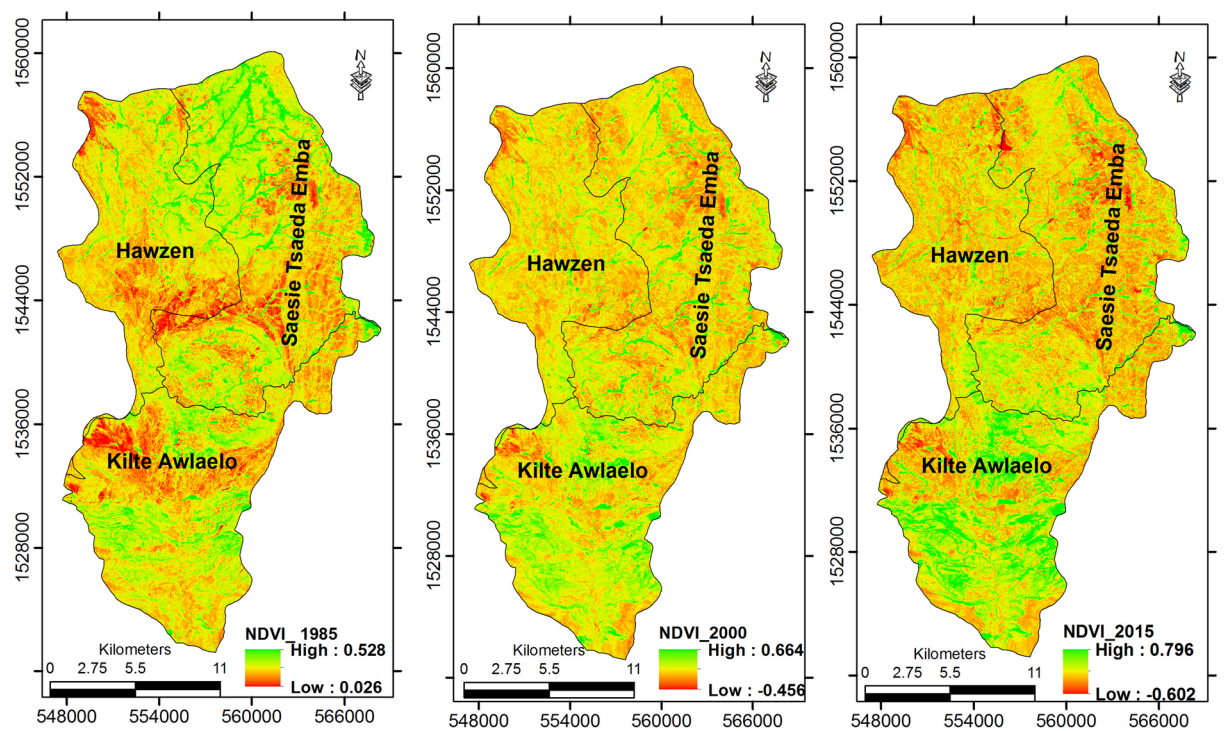

Fig. 2 NDVI results of Middle Suluh River Basin for 1985, 2000 and 2015

spectrum to analyze whether the target area contains live green vegetation or not. Healthy vegetation absorbs most of the visible light that falls on it, thereby reflecting a large portion of the NIR.

As listed in Table 1, all the Landsat images were obtained from United States Geological Survey (USGS), http://earthexplorer.usgs.gov and were analyzed and presented using ENVI 5.3 and ArcGIS 10.3 to classify the vegetation density in terms of NDVI and SAVI in the study area.

Figure 2 shows the spatial distribution of normalized difference vegetation index (NDVI) for the Middle Suluh River Basin based on comparison of Landsat images at three times (26 February 1985, 15 March 2000 and 13 February 2015). The provided dates offer the best cloud free moments after the harvest season so that the extraction of reflectance just from vegetation cover is possible which is appropriate to fetch the required data. The normalized difference vegetation index (NDVI) is one of the standardized indices that uses the combination of the red (0.63–0.69 μm) reflectance and near infrared (0.76–0.90 μm) reflectance of the electromagnetic spectrum and defined as:

$$NDVI = \frac{NIR - R}{NIR + R} \tag{1}$$

The NDVI value falls between − 1 and + 1, where increasing positive values indicate increasing green vegetation and negative values indicate non-vegetated surface features such as water, barren land, ice, snow, or clouds (Sahebjalal and Dashtekian 2013). The NDVI of 1985 indicates that there was more vegetation cover in the northern part than in the middle and southern part of the study area. However, in 2000, the density of greenness radically decreased in the northern part while it improved towards the southern section of the study area. In 2015, the density of greenness showed a dramatic increase in the southern part where parts of *Kilte Awulaelo* district is located (Fig. 2). During field observation, it was learned that in this part of the valley free grazing was prohibited by community agreed by-laws.

Retrieval of LST from Landsat images

Conversion of DN values into radiance

All Landsat TM bands are quantized in 8-bit data format. Hence, these data are recorded in the form of digital numbers (DN) ranging between 0 and 255. By extracting some important information from the metadata, the conversion from DNs to top of atmospheric (ToA) reflectance for the TM band requires using a two-step process. On the other hand, the Landsat 8 OLI sensor is more sensitive so the raw data are rescaled into 16-bit DNs with a range from 0 and 65,536, requiring its conversion in a single step. Finally, for any of the bands, the reflectance values range from 0.0 to 1.0 and are stored in floating point data format. However, in this study ENVI 5.3 software was used for all bands (TM and OLI) to convert the DN values into reflectance using the reflectance tool under the radiometric calibration (RC) toolbox. First, these data were converted into radiance values using the NASA (2009), Chander et al. (2009).

$$L_\lambda = \left(\frac{(LMAX_\lambda - LMIN_\lambda)}{(QCALMAX - QCALMIN)}\right) * (QCAL - QCALMIN) + LMIN_\lambda \tag{2}$$

where, L_λ: spectral radiance at the sensor's aperture in watts/(meter squared * ster * μm); QCAL: the quantized calibrated pixel value in DN; $LMAX_\lambda$: the spectral radiance scaled to QCALMAX in watts/(meter/squared * ster * μm); $LMAX_\lambda$: the spectral radiance scaled to QCALMAX in watts/(meter/squared * ster * μm); QCALMIN: the minimum quantized calibrated pixel value (typically 0 or 1); QCALMAX: the maximum quantized calibrated pixel value (typically = 255).

Conversion of radiance to brightness

Spectral band brightness temperature (BT) is the temperature a blackbody needs to have to emit a specified radiance for a given sensor band (Berk 2008). By applying the inverse of the Planck function, thermal bands' radiance values were converted into brightness temperature values using the following equation (Chander et al. 2009).

$$\mathrm{T} = \frac{K_2}{\ln\left(\frac{K_1}{L\lambda} + 1\right)} \tag{3}$$

where, T: at-satellite brightness temperature (K); L_λ: TOA spectral radiance (watts/(m^2 * srad * μm)); K_1: band-specific thermal conversion constant from the metadata (K1_CONSTANT_BAND_x, where x is the thermal band number); K_2: band-specific thermal conversion constant from the metadata (K2_CONSTANT_BAND_x, where x is the thermal band number).

Conversion of radiance to reflectance

By converting the spectral radiance to planetary reflectance, or albedo, a reduction in between-scene variability can be achieved through normalization for solar irradiance. Radiances are converted to reflectance using the Sun zenith angle cosine interpolated at the pixel and the Sun spectral flux. The combined surface and atmospheric reflectance of the Earth is computed with the equation recommended by Chander et al. (2009).

$$\rho_p = \frac{\pi \cdot L_\lambda \cdot d^2}{ESUN_\lambda \cdot \cos\theta_S} \tag{4}$$

where, ρ_λ: unit less planetary reflectance; L_λ: spectral radiance (from earlier step); d: Earth–Sun distance in astronomical unit; $ESUN_\lambda$: mean solar exo-atmospheric irradiances; θ_s: solar zenith angle.

Estimating proportion of vegetation and emissivity

In this study, the semi-automatic classification plug integrated with open source GIS package (QGIS 2.18) was used for image acquisition, pre-processing and deriving brightness temperature to be used for final LST computation. Land surface emissivity is an average emissivity of an element of the surface of the Earth calculated from measured radiance and land surface temperature (LST). In order to calculate land surface emissivity, understanding the proportion of vegetation or vegetation fraction from the NDVI output is essential. Carlson and Ripley (1997) defined the proportion of vegetation with the following equation:

$$Pv = \left(\frac{NDVI - NDVI_{min}}{NDVI_{max} - NDVI_{min}}\right)^2 \quad (5)$$

where, $NDVI_{min}$, and $NDVI_{max}$, correspond to the values of NDVI minimum and NDVI maximum in an image, respectively. Sobrino and Raissouni (2000) and Valor and Caselles (1996) used different approaches to predict land surface emissivity from NDVI values. Sobrino et al. (2004) have developed a better equation to compute the land surface emissivity using the mean value for the emissivity of soils included in the ASTER spectral library (http://asterweb.jpl.nasa.gov) as indicated below:

$$\varepsilon mmisivity = 0.004Pv + 0.986 \quad (6)$$

Weng (2009) noted that emissivity for ground objects from passive sensors like Landsat has been estimated using different techniques such as the (1) NDVI method; (2) classification-based estimation, and the (3) temperature-emissivity separation model. These techniques are applicable to separate temperature from emissivity, so that the effect of emissivity on estimated LST's can be determined. Hence for this study, Eq. (6) shows that surface emissivity on pixel based remote sensing is derived using the NDVI method in conjunction with proportional vegetation (Pv) cover (Valor and Caselles 1996).

LST is very important not only for soil development and erosion studies, but also to estimate amounts of vegetative cover and land cover changes (Li et al. 2013). This is because the natural phenomena on the Earth's surface have no homogeneous characteristics in terms of land surface emissivity. It is true that surface emissivity is highly dependent on the type of vegetation cover, roughness of the topography and soil and mineral composition of the Earth surface.

Using this approach, the land surface emissivity of the three Landsat images (1985, 2000 and 2015) were calculated for further computation of land surface temperature (LST) of the study area. The LST results are all in degree celsius. For Landsat 5 (year 1985) and Landsat 7 ETM+ (year 2000), band 6 was used from the Thermal Infrared Sensor. For Landsat 8 OLI (year 2015), bands 10 and 11 from the thermal infrared sensor (TIRS) were also used. The land surface temperature (LST) is the radiative skin temperature of the ground which depends on albedo, vegetation cover and soil moisture of the land surface (Suresh et al. 2016).

Land surface temperature (LST)

A series of satellite and airborne sensors have been developed to collect TIR data from the land surface, such as Landsat TM/ETM+/OLI, AVHRR, MODIS, ASTER, and TIMS (Al-doski et al. 2013; Weng 2009). The measurement of LST could be affected by the differences in temperature between the ground and vegetation cover. The brightness temperatures from TM band 6 thermal for the years 1985 and 2000 Landsat images, OLI band 10 and 11 for year 2015 Landsat image were used to calculate the emissivity corrected LST using Eq. (7), as used in Sobrino et al. (2004), Weng et al. (2004) and Yue et al. (2007).

$$LST = BT/(1 + W * (BT/P) * \ln(e)) \quad (7)$$

where, LST: land surface temperature; BT: at-sensor brightness temperature (K); P: 14,380; W: wavelength of emitted radiance (11.5 μm); Ln(*e*): log of the spectral emissivity value.

Soil adjusted vegetation index

The spectral reflectance of plant canopy is a combination of the reflectance spectra of plant and soil components (Rondeaux et al. 1996) which makes researchers interested to develop new indices like SAVI. This index is a measure of healthy, green vegetation which is similar to NDVI, but it suppresses the effects of soil pixels. The notable improvement of this index by Huete (1988) led again to further development of transformed soil adjusted vegetation index by Baret and Guyot (1991). The soil-adjusted vegetation index was developed to correct the influence of soil brightness when vegetative cover is low. According to Huete (1988), L is assumed a correction factor and its value is dependent on the vegetation cover. Total vegetation cover that receives a value of zero, it effectively turns SAVI into NDVI. For very low vegetation cover, it receives the value of 1. In this manner, Huete developed a three point adjustments as optimal for the L constant ($L = 1$ for low vegetation densities; $L = 0.5$ for inter-mediate vegetation densities; $L = 0.25$ for higher densities). In support this, Aboelghar et al. (2014) and Badreldin and Goossens

(2015) argued that L = 0.5 successfully minimizes the impact of soil variations in green vegetation compared to NDVI. Hence, for the purpose of this study, we used 0.5 to represent intermediate vegetation cover in such semi-arid environment using the following equation:

$$SAVI = \frac{(NIR - R)}{(NIR + R + 1)} * (1 + L) \quad (8)$$

The AAP was computed for long-term seven gauge stations distributed within and outside the study area from 1973 to 2015. Using the spatial analyst tool in ArcGIS, inverse distance weight (IDW) interpolation technique was employed to generate a surface of mean precipitation on pixel basis. These data were then used for further regression analysis to examine relationships with the SAVI results.

Results and discussion

Interpretation of AAP distribution and SAVI

For better understanding of the SAVI, LST and AAP pattern and relationships in the study area, the computed results were displayed simultaneously in ArcGIS 10.3. The figures highlight a visual illustration of the spatial pattern of thermal environment, vegetation cover and long term AAP distribution in the study area. The spatial distribution of the highest averages of annual precipitation (Fig. 3 on top) increased from 756 mm in 1973–1985 to 857 mm in 1986–2000 period. As we can observe from Fig. 3, the spatial coverage's of extensive precipitation in the study area was observed in the period of 1986–2000. In this period, the less extensive coverage's of precipitation is observed in the western part of the study area in part of *Hawzen* district. The highest AAP has again decreased from 856 mm in 1986–2000 to 621 mm in 2001–2015. In the last period, extensive part of the study area received low AAP compared to the periods in 1973–1985 and 1986–2000 (Fig. 3 top).

From Fig. 3 (bottom) it can be revealed that there was high density of SAVI coverage in 1985 mainly in the northern part of the study area. This area was characterized with more of flat topography covered with grasses and gradually converted into agricultural lands. In the middle part where there is more exposed granitic rocks at the ground shows less density of SAVI while it slightly increases in the southern part. After 15 years in 2000, the SAVI distribution shows low density throughout, while it shows a relatively increase in the southern part of the study area. In 2015, the highest density of SAVI was distributed in the southern part of the study area (Fig. 3, bottom) where high vegetation restoration was observed during conducting the fieldwork assessment. During the discussion made with the village administrators and agricultural development agents, they have agreed that the improvement is in the effect of community based SWC activities. One of the villages located in the study area called *Abraha Atsibaha* was evidenced as winner of the 2012 UNDP Equator Prize at Rio de Janeiro in recognition of outstanding success to restoration of degraded landscape through SWC practices (Kahsai 2015).

The soil and water conservation practices implemented in the study area have thus resulted in a better restoration of the natural environment. Figure 5a shows the degraded and heavy gully formation in *Kilte Awulaelo* district, *Abraha Atsibaha* village in 2006. After intensive intervention of community based SWC practices on the hillside (Fig. 5c), the degraded landscape started to recover its vegetation density (Fig. 5b). The mean SAVI of this specific village shows significant increment from 0.16 in 1985 to 0.18 in 2000 and reached 0.19 in 2015 (Fig. 4). Places like *Frewyni* town have shown declines in SAVI since 1985 for its conversion of land into urban functions (Fig. 4). In most of the properly conserved areas, farmers benefited directly or indirectly from the conserved resources. For example, Fig. 5d shows a good structured communal well recharged underground water and used for irrigation of nearby farmlands.

Similarly in Fig. 5e, a woman is harvesting grass from the area exclosure for cattle feed. In *Abraha Atsibaha* and *May Kuha* villages where the highest mean SAVI values are observed, free grazing was seriously restricted. Farmers have set their own communal resource use bylaw locally called "*Sirit*", and practically implemented it in the area. Therefore, zero grazing was used as the most beneficial land rehabilitation mechanism and farmers are allowed to harvest grasses without limit from all area exclosures, hillside terraces and other protected areas. Park et al. (2013) addressed that area exclosure is one of SWC practice considered a well-known management tool to restore vegetation cover and in turn increase soil organic matter.

In order to assess the increment of vegetation cover, only SAVI values ≥ 0.2 were extracted as recommended by experts (see at https://phenology.cr.usgs.gov/ndvi_foundation.php). The result in Fig. 6 shows that in 1985, the total land area with SAVI ≥ 0.2 was 23.57 km^2. After 15 years (2000), the total area covered with vegetation amounting SAVI ≥ 0.2 increased to 64.94 km^2, which is over a twofold increase from the 1985 SAVI. In 2015, the total area with a SAVI value of ≥ 0.2 reached 67.11 km^2 (Fig. 6), which shows a 3.3% increment from year 2000 value. These changes are attributable to the soil and water conservation interventions guided by the environmental rehabilitation strategy of the Regional State of Tigray.

In general, the average annual increment rate observed over a period of 30 years (1985–2015), using SAVI image, was 6.2%. The vigorous SWC activities performed throughout country are also evidenced by EBI (2014) for

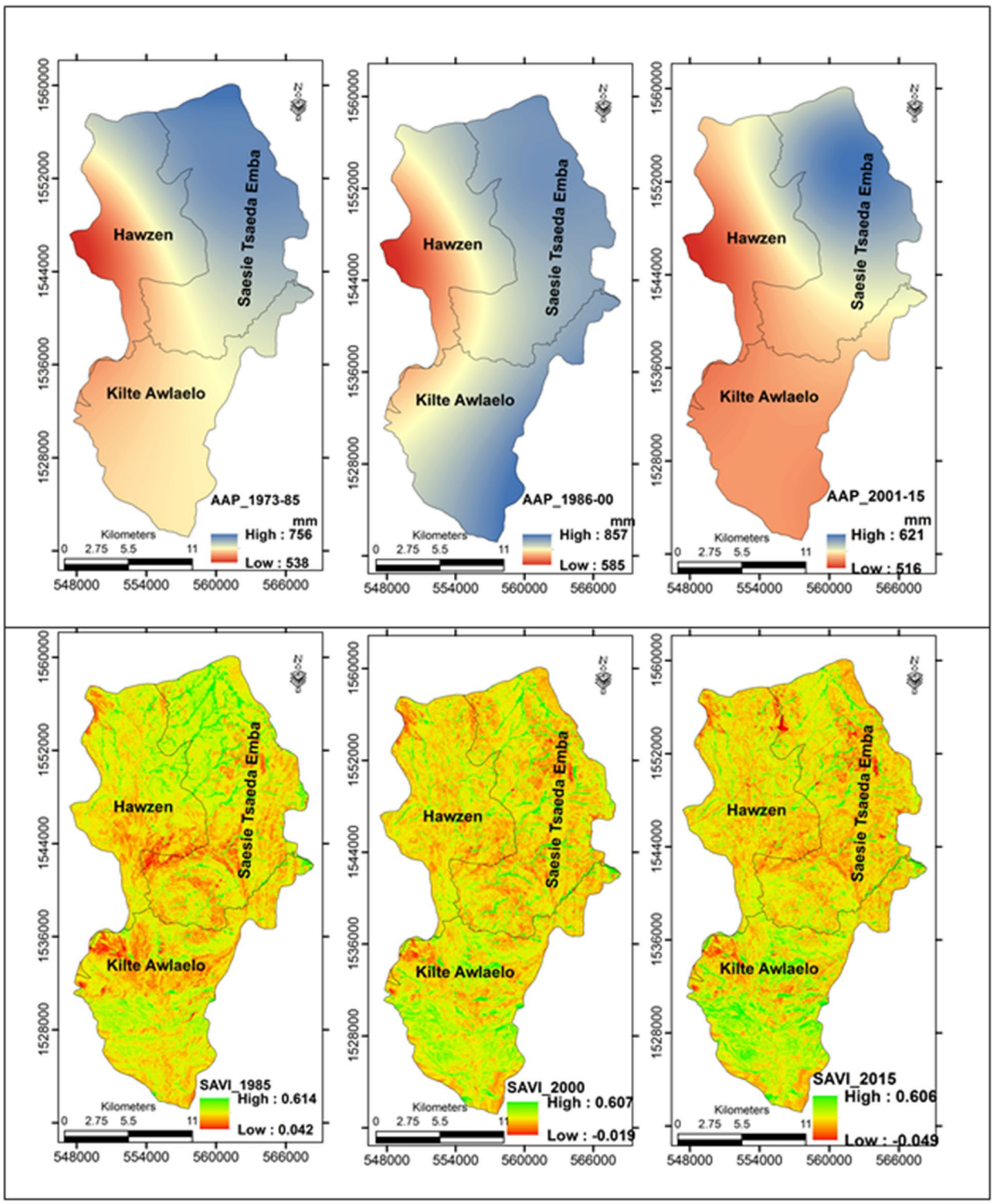

Fig. 3 IDW interpolation of average annual precipitation (top) and SAVI (bottom) for 1985, 2000, and 2015

the rehabilitation and restoration of degraded areas. This resulted in increased vegetation cover and enhancement of biodiversity.

Interpretation of LST and SAVI

Maximum LST has reduced from 42.2 °C in 1985 to 36.7 °C in 2015. This could be due to the improvement in

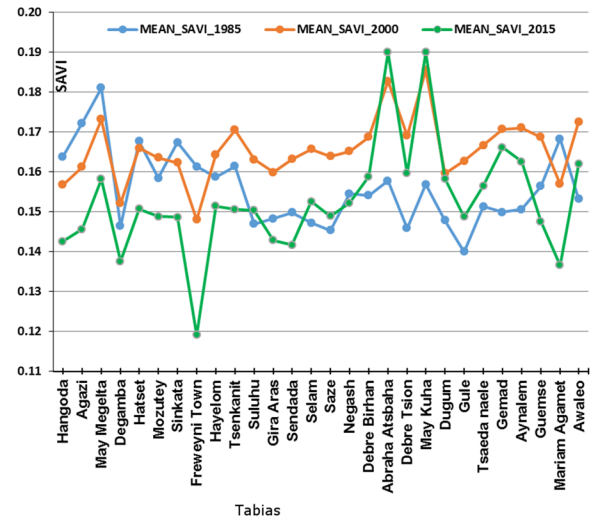

Fig. 4 Mean SAVI distribution in the village polygons in 1985, 2000 and 2015

the surface vegetation cover. Similar studies by Alshaikh (2015) and Sun et al. (2012) revealed that areas with rich vegetation cover have characterized by lowest LST. In Fig. 7 (top), the lowest LST distribution was also mainly observed in areas indicated by fairly high AAP in *Saesie Tsaeda Emba* district. In 2000 and 2015, the lowest LST were found in areas where more vegetation cover was observed in the southern part of the study area.

Relationship of NDVI with LST and vegetation abundance

The concept of LST–NDVI space was first formulated by Lambin and Ehrlich (1996) with LST plotted as a function of NDVI. As indicated in Fig. 8, modified by Sandholt et al. (2002), the left edge represents bare soil from dry to wet (top–down) range. Along the X-axis, as the amount of green vegetation increases, the NDVI value also increases and inversely the maximum LST decreases. As indicated in Fig. 8 for the dry conditions, the negative relationship between LST and NDVI is defined by the upper edge, which is the upper limit of LST for a given type of surface and climatic conditions (Sandholt et al. 2002).

The relationship between NDVI and LST was investigated for each period (1985, 2000, and 2015) through regression analysis. The regression was performed from the mean values extracted in the zonal statistics in ArcGIS. Within the study river basin, there are 28 *tabias* situated some fully and some partially within the boundary.

A regression of NDVI_2015 as a dependent and LST_2015 as an independent variable was carried out. The linear regression established between LST_2015 and NDVI_2015 was statistically significantly ($p < 0.05$). The regression model indicates that 18.31% of the variation in mean NDVI_2015 was explained by the LST_2015 (Fig. 9a). The regression equation was modelled as NDVI_2015 = 0.615 − 0.013 LST_2015. The result shows that there is significant inverse correlation between NDVI and LST in all the periods (Fig. 9a–c; Table 2).

Similarly, a regression of NDVI in 2000 as dependent and LST in 2000 as an independent variables was carried out. The linear regression established shows that LST is statistically inversely significantly predicted NDVI, $F(1,26) = 18.21$, $p < 0.0005$, (= 0.000) and LST accounted for 64% of the explained variability in NDVI. The regression equation was expressed as NDVI_2000 = 0.557 − 0.01 LST_2000 (Table 2).

For 1985, a linear regression was run to predict NDVI in Landsat images from LST of similar period. The independent variable (LST) has statistically significantly predicted NDVI, $F(1,26) = 8.6$, $p < 0.05$, $R^2 = 0.249$. The LST accounted for 22.9% of the explained variability in NDVI. The regression equation has been derived as NDVI_1985 = 0.375 − 0. 005 LST_1985 (Fig. 9c).

As Evans (1996) suggested for the value of *r*, the Pearson correlation coefficient in 2000 shows a strong correlation between NDVI and LST (Table 2). In the year 1985 and 2015, the correlation coefficient was classified as a moderate correlation between NDVI and LST. Similar results were attributed for the relationship between NDVI and LST by Yue et al. (2007) using Landsat 7 ETM+ data in Shanghai, and by Sahana et al. (2016) using Landsat 5 TM and Landsat 8 OLI in the Sundarban Biosphere Reserve, India; Karnieli et al. (2010).

Relationship of SAVI with LST using village polygons

The different SWC measures applied in the study area have also significance to the improvement of vegetation cover. In order to detect the vegetation cover dynamics, a SAVI model formulated by Huete (1988) was preferred. This model best fits for a semi-arid environment to reduce the afterward influence of soil in considering soil coefficient of 0.5. Likewise for 1985, 2000, and 2015 (Fig. 10), SAVI was computed from Landsat images taken in the months of February and March and its relationship with LST was compared.

Accordingly, a regression of SAVI in 1985 as a dependent and LST in 1985 as an independent variable was carried out to see the relationship. The linear regression established shows that LST is statistically inversely significant predicted SAVI, $F(1,26) = 10.3$, $p < 0.005$, (= 0.004) and LST accounted for 28.3% of the explained variability in SAVI. The regression equation was derived as SAVI_1985 = 0.275 − 0.004 LST_1985.

Likewise, a simple linear regression was conducted to exhibit the relationship between SAVI and LST for every village polygons in the year 2000. The results are shown

Fig. 5 Rehabilitation of degraded landscape and its benefit to local farmers. **a** Heavy gully observed in 2006 from google Earth (Kilte Awulaelo district, village Abraha Atsibaha); **b** restored gulley in 2016 photo from google Earth (Kilte Awulaelo district, village Abraha Atsibaha); **c** conserved hillside (Kilte Awulaelo district, village Abraha Atsibaha, photo: researcher); **d** ground water harvesting at the bottom of the hill (Hawzen district, Hayelom village, photo: Hawzen district office of agriculture and rural development (HDOARD); **e** a woman harvesting grass in area exclosure (Kilte Awulaelo district, Abraha Atsibaha, photo: researcher); **f** potato harvesting from irrigated land (Saesie Tsaeda Emba district, *Saz* village, photo: researcher)

in Table 2 where Y is the mean SAVI associated with the village polygons and X is LST associated with the village polygons constructed under zonal statistics in ArcGIS software. The result indicates that at 95% confidence interval, LST is statistically significant predicted SAVI, $F(1,26) = 9.06$, $p < 0.05$, (= 0.006) and LST accounted for 25.8% of the explained variability in SAVI. The regression

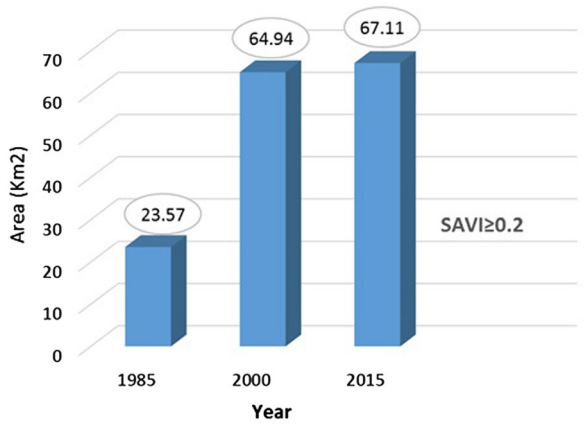

Fig. 6 SAVI area coverage in 1985, 2000, and 2015

equation was presented as SAVI_2000 = 0.282 − 0.003 LST_2000.

The relationship between SAVI and LST for the period of 2015 was also computed. The significant regression was checked through a *t*-test α = 0.05. The result revealed that there was not statistically significant predicted SAVI, $F(1,26) = 2.67$, $p > 0.05$, (= 0.114) and LST accounted for only 5.83% of the explained variability in SAVI which is relatively lower than in the year 1985 and 2000. The fitted line plot for the linear model was SAVI_2015 = 0.279 − 0.004 LST_2015. Like the NDVI and LST relationship tested previously, SAVI also exhibited an inverse relationship with LST. This was similar with the result found by Badreldin and Goossens (2015) who studied for monitoring mitigation strategies effects on desertification change in an arid environment. This means that areas with high vegetation density are represented with a low surface temperature and vice versa.

With the Pearson's correlation classes suggested by Evans (1996) there was negatively weak relationship between SAVI and LST in 2015 and where as in the year 1985 and 2000, a negatively moderate relationship was observed (Fig. 10a–c; Table 2).

Relationships between SAVI and LST; SAVI and AAP pixel by pixel

SAVI as a measure of vegetation restoration was computed to test the relationship with LST and AAP pixel-by-pixel. Table 3 shows that the Pearson's correlation coefficients between SAVI and AAP; SAVI and LST over the years 1985, 2000 and 2015. It is evident from Fig. 10 that LST values tend to negatively correlate with SAVI values for all study periods. The highest negatively correlation (− 0.359) was found in the year 2000 and the lower negatively correlation (− 0.102) was observed in the year 1985 (Table 3). According to Evans (1996) correlation strength classification, in years 2000 and 2015, the relationship between SAVI and LST shows negatively weak correlation and whereas in 1985 was negatively very weak correlation. The negative correlation between LST and SAVI implies that areas with lower biomass of the vegetation have higher LST and vice versa. The combination of LST and SAVI by scatterplot results in a triangular shape like LST and NDVI as described by other scholars (see for example Carlson et al. (1994); Gillies et al. (1997); Gillies and Carlson (1995); Weng et al. (2004)).

All the models are statistically significant ($p < 0.05$) and the pixel based samples were large enough (n = 544365) to obtain a precise estimate of the strength of the relationship. In the year 2015 the previously observed highest vegetation density indicated with 1.8% of the variation can be accounted for by the regression model (Fig. 11a). A significant negative correlation ($r = -0.135$; $p < 0.05$) was found between the pixel based mean SAVI and pixel based AAP, which indicates that as AAP in 2015 decreases, SAVI 2015 tends to increase. On the contrary, the very weak positive correlation ($r = 0.057$; $r = 0.252$) in the year 2000 and 1985 respectively indicates that when APP increases, SAVI also tends to increases to some extent (Table 3).

However, the significant increase of vegetation density in the study area could be due to other factors: (1) effect of appropriate SWC practices implemented to rehabilitate the degraded landscape; (2) vegetation water use efficiency; (3) the impact of zero grazing for protection of area exclosure. In a Reuters news report written by Whiting (2017) as cited from Chris Reij, desertification expert at the World Resources Institute, addresses that the Tigray Region of Ethiopia is now greener than it has ever been during the last 145 years and the improvement of the vegetation cover is not due to an increase in rainfall, but due to human investment in restoring degraded land to productivity. For this reason, Ethiopia's Tigray Region won gold in a U.N.-backed award in 2017 for the world's best policies to combat desertification and improve fertility of dry lands (Whiting 2017). Davenport and Nicholson (1993) observed the notable inconsistencies in the vegetation index and rainfall associations that argued the relationships between precipitation and NDVI are not direct and causal. Contrarily, Kassie et al. (2008) argued that physical-based SWC measures did not have a positive impact but reduced yield and biomass in the high-rainfall areas of the Ethiopian highlands compared with non-conserved plots.

Conclusions

Studies revealed that SWC has been implemented in the Tigray Region, of northern Ethiopia since 1985. The implementation was more effective from the early

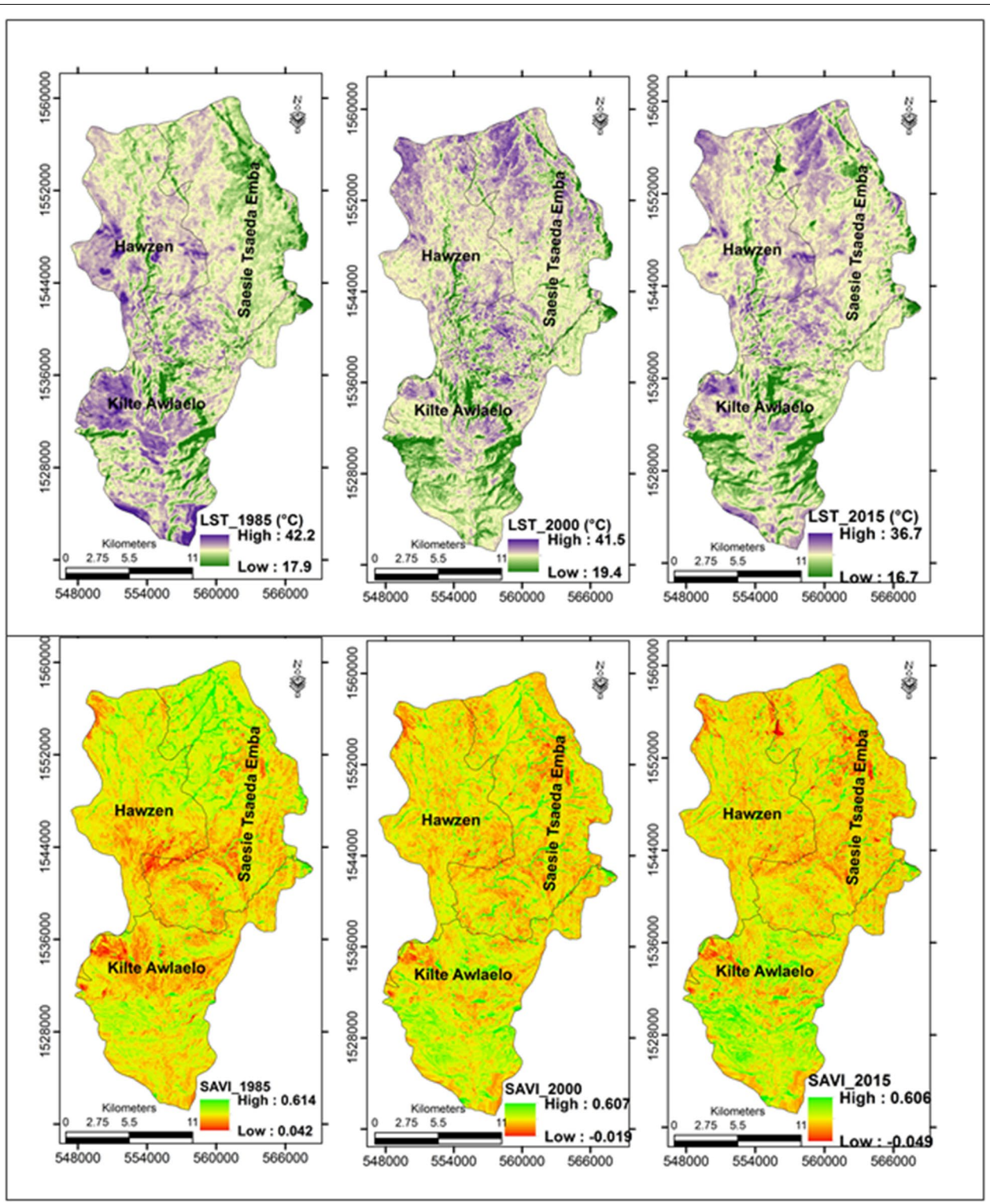

Fig. 7 LST results for 1985, 2000 and 2015 (top); SAVI results for 1985, 2000, and 2015 (bottom)

90s due to the more emphasis given by the government towards land rehabilitation. The implementation of SWC in the region as a strategy was to reduce run-off, improve soil fertility and finally reverse the degraded landscape for the betterment of the rural livelihood. This study evaluated changes in vegetation cover following

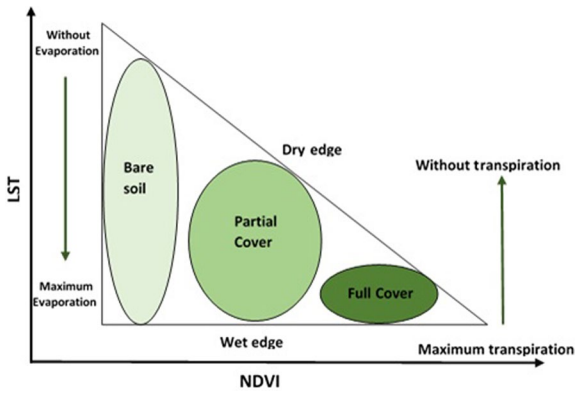

Fig. 8 Simplified LST/NDVI (Reproduced with permission from Lambin and Ehrlich 1996; Sandholt et al. 2002)

the implementation of SWC measures. Satellite images were used to generate SAVI and LST, whereas long-term AAP records were also used to account for the effects of precipitation. The implementation of different forms of SWC activities, such as area exclosure, stone terraces, soil bunds, contour ditches, moisture retention reservoirs and check dams are an optimal solution to reverse the vegetation degraded landscape of arid and semi-arid regions in Ethiopia. The supplemental survey made in the study area asserts that 95% of the respondents observed a vegetation cover improvement in their locality over the last 25 years. This was due to the proper implementation of SWC, particularly the practice of area exclosure in protecting from human and livestock interference for better restoration. When degraded landscape protected

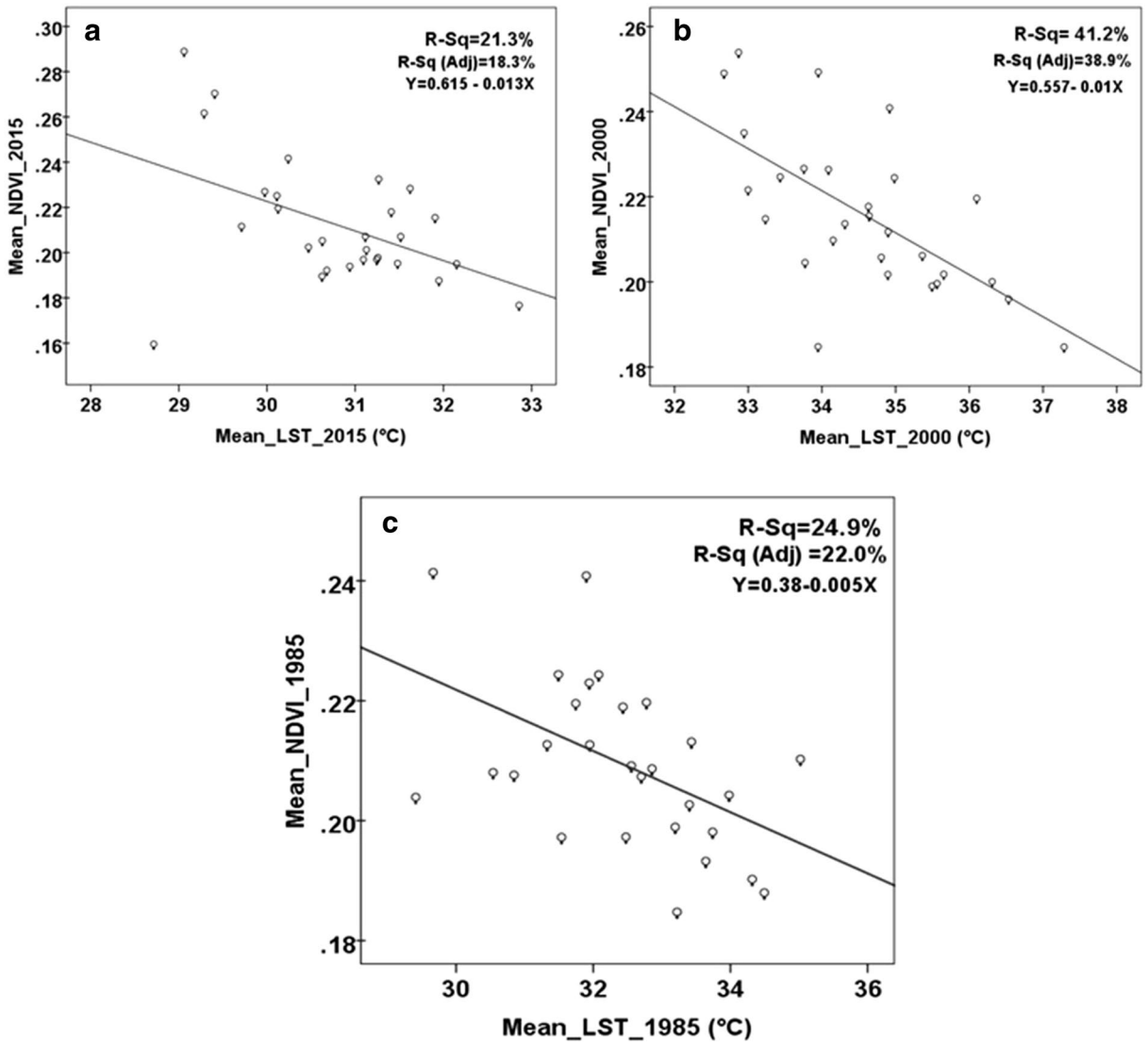

Fig. 9 The mean LST and SAVI relationship over years 1985, 2000 and 2015 at village polygons. **a** regression plot between mean NDVI of 2015 and mean LST of 2015; **b** regression plot between NDVI of 2000 and mean LST of 2000; and **c** regression plot between NDVI of 1985 and LST of 1985 (all at village polygons)

Table 2 Linear regression and correlation coefficients for the relationship between LST and SAVI in 1985, 2000, and 2015

Dependent variable	Independent variable	Regression equation	R^2 (%)	R^2 adjusted	*r*	*Sig.*
NDVI_2015	LST_2015	Y = 0.615 − 0.013x	21.3	18.31	− 0.46	0.013
NDVI_2000	LST_2000	Y = 0.557 − 0.010x	41.2	38.92	− 0.64	0.000
NDVI_1985	LST_1985	Y = 0.375 − 0.005x	24.9	21.97	− 0.50	0.007
SAVI_2015	LST_2015	Y = 0.275 − 0.004x	9.3	5.83	− 0.31	0.114
SAVI_2000	LST_2000	Y = 0.282 − 0.003x	25.8	22.99	− 0.51	0.006
SAVI_1985	LST_1985	Y = 0.275 − 0.004x	28.3	25.53	− 0.53	0.004

SAVI soil adjusted vegetation index, *LST* land surface temperature, *NDVI* normalized difference vegetation index

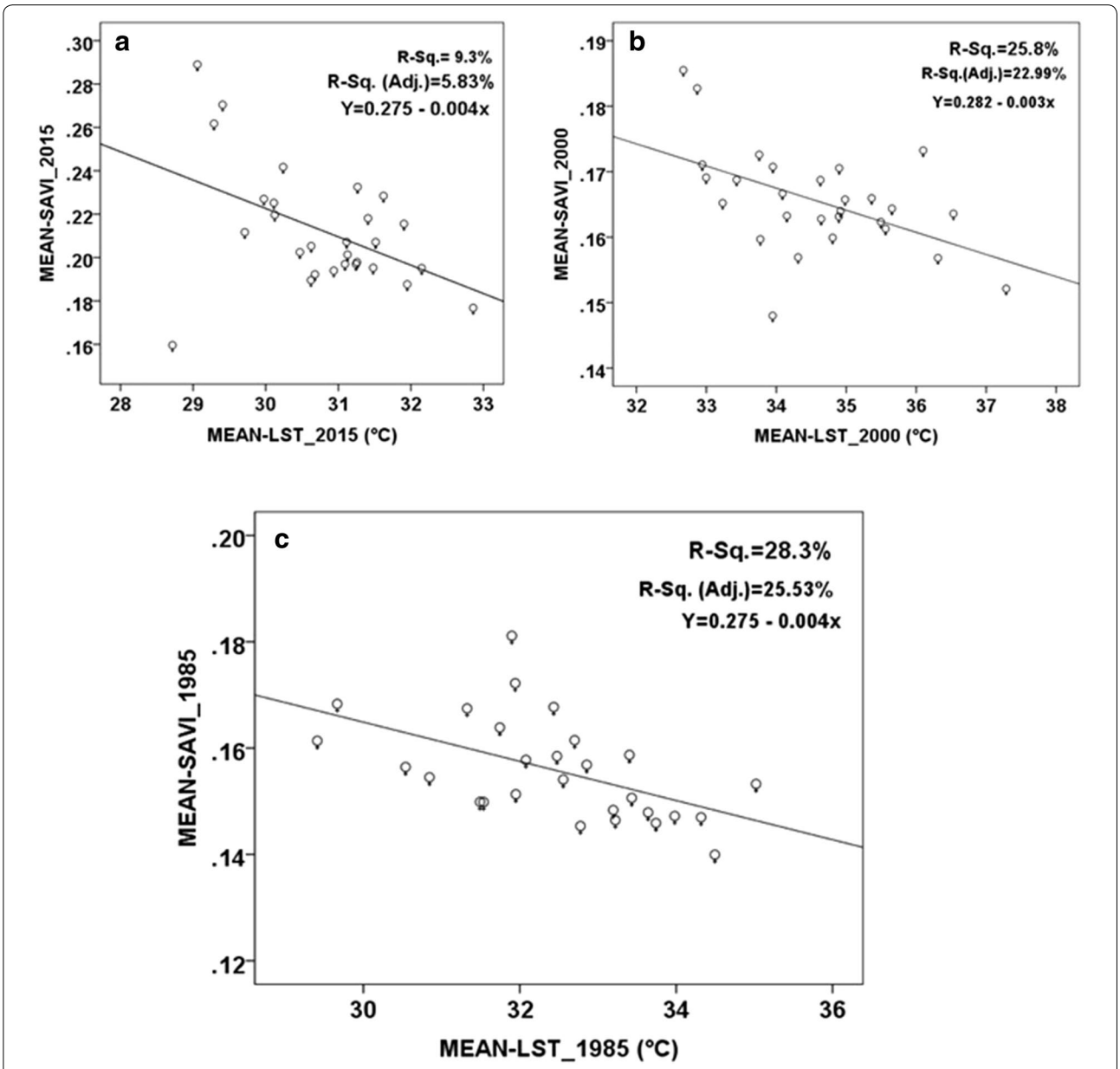

Fig. 10 Linear regression of mean SAVI and mean LST by village's polygon over years 1985, 2000, and 2015. **a** regression plot of mean SAVI 2015 and mean LST 2015; **b** regression plot between mean SAVI of 2000 and LST of 2000; and **c** regression plot of mean SAVI 1985 and mean LST 1985 (all at village polygon)

Table 3 Linear regression and correlation coefficients for the relationship between SAVI and LST; SAVI and AAP in 1985, 2000, and 2015 pixel-by-pixel

Dependent variable	Independent variable	Regression equation	R^2 (%)	R	*r*	Sig.
SAVI_2015	LST_2015	Y = 0.331 − 0.0057x	7.2	0.269	− 0.269	0.000
SAVI_2000	LST_2000	Y = 0.352 − 0.0052x	12.9	0.359	− 0.359	0.000
SAVI_1985	LST_1985	Y = 0.193 − 0.0011x	1.0	0.102	− 0.102	0.000
SAVI_2015	AAP[a]	Y = 0.287 − 0.0002x	1.8	0.135	− 0.135	0.000
SAVI_2000	AAP[b]	Y = 0.138 − 0.00004x	0.3	0.057	0.057	0.000
SAVI_1985	AAP[c]	Y = 0.051 − 0.0002x	6.4	0.252	0.252	0.000

[a] Average annual precipitation for 2015

[b] Average annual precipitation for 2000

[c] Average annual precipitation for 1985

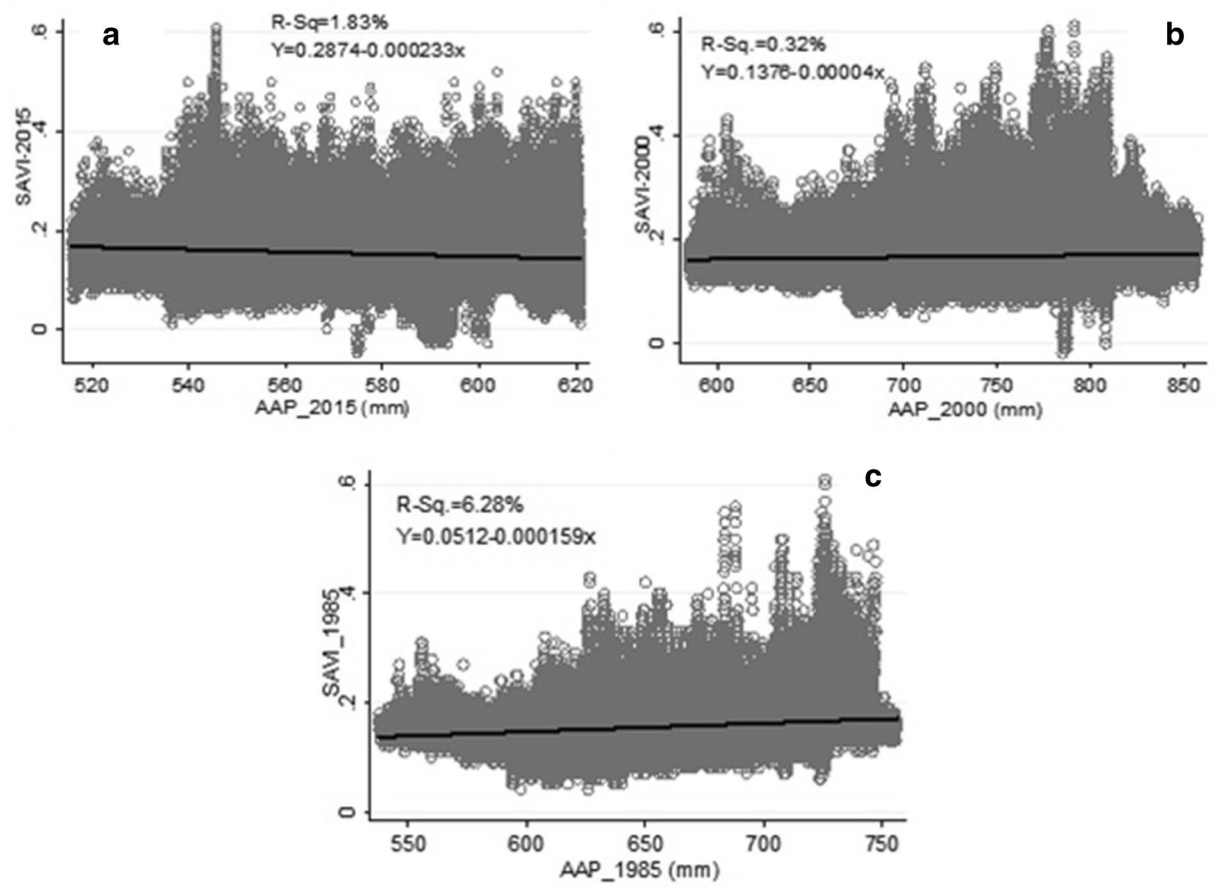

Fig. 11 Scatter plot of linear regression model between SAVI and AAP in 1985, 2000 and 2000 pixel-by-pixel. **a** regression plot of SAVI 2015 and AAP 2015; **b** regression plot of SAVI 2000 and AAP 2000; and **c** regression plot of SAVI 1985 and AAP 1985 (all pixel-by-pixel).

with different SWC practices, run-off will reduce, infiltration capacity will increase, which retain soil moisture and finally improve vegetation density. In order to achieve such results, the involvement of local communities at all processes in the conservation program is essential. On this matter, Bewket (2007) argued that the success of any SWC intervention depends on the extent to which the introduced conservation technologies are accepted and adopted by the farmers.

The pixel-by-pixel correlation between SAVI and long-term AAP explained better estimates as compared to the village polygon results. Even though the AAP

distribution shows a declining trend over the 30 years of study period, the vegetation cover shows an increasing trend. This was proved statistical inversely significant correlation between SAVI and AAP ($r = -0.135$) in the year 2015. This clearly indicates that the significant increase in vegetation cover was not the result of precipitation rather other factors like the integrated SWC practices applied in the area contributes significantly. When appropriate SWC techniques were applied, runoff can be reduced and instead the infiltration rate and water holding capacity of the soil can be improved. To assert such a result, similar studies shall be done in other SWC practiced areas and their results will be compared for a better conclusion.

It is recommended that the implementation, protection and follow-up of SWC activities require the direct involvement of rural communities at all stages for the better and sustainable restoration of vegetation cover. The study has shown that SAVI and LST derived from Landsat images in different periods, and AAP of long-term station measurements are useful data when analyzing the relationship between precipitation and vegetation cover and detecting vegetation cover improvement.

Authors' contributions
SH has made substantial contribution in conception design, acquisition of data, interpretation of results and leading the overall activities of the research; WB and JL have been involved in guiding the principal author and critically commenting the manuscript. Both have given approval of the current version to be published. All authors read and approved the final manuscript.

Author details
[1] Department of Geography and Environmental Studies, Mekelle University, P.O. Box 231, Mekelle, Ethiopia. [2] Institute of Resources Assessment, University of Dar es Salaam, Dar es Salaam, Tanzania. [3] Department of Geography and Environmental Studies, Addis Ababa University, Addis Ababa, Ethiopia.

Acknowledgements
The authors would like to thank TRECCAfrica II for providing scholarship to the corresponding author to study Ph.D. programme at the Institute of Resources Assessment, University of Dar es Salaam, Tanzania. The USGS website that allowed the authors to download the Landsat images freely from their archives should also be acknowledged. The authors would also like to thank the Metrological agency of Mekelle branch for providing us climatic data; and local community of the study area for their cooperation during the fieldwork. Moreover, many thanks to Dr. Haile Muluken and Mr. Ramzy Bejjani for proof reading and editing the manuscript. Finally, special thanks go to the anonymous reviewers which helped to improve this manuscript.

Competing interests
The authors declare that they have no competing interests.

Availability of data and materials
Authors declare that the data and materials presented in this manuscript can be made publically available by Springer Open as per the editorial policy.

Consent for publication
Not applicable.

Ethics approval and consent to participate
Not applicable.

Funding
The first author is also grateful to Mekelle University for granting research fund under Registration Number CRPO/CSSL/PhD/003/08; and to Association of African Universities (AAU) for awarding small grants for thesis writing.

Publisher's Note

Received: 25 May 2017 Accepted: 28 November 2017
Published online: 21 December 2017

References
Aboelghar M, Ali A, Arafat S (2014) Spectral wheat yield prediction modeling using SPOT satellite imagery and leaf area index. Arabian J Geosci 7:465–474. https://doi.org/10.1007/s12517-012-0772-6

Al-doski J, Mansor SB, Zulhaidi H, Shafri M (2013) NDVI differencing and post-classification to detect vegetation changes in Halabja City, Iraq. J Appl Geol Geophys 1(2):1–10

Alshaikh A (2015) Vegetation cover density and land surface temperature interrelationship using satellite data, case study of Wadi Bisha, South KSA. Adv Remote Sens 4:248–262

Badreldin N, Goossens R (2015) A satellite-based disturbance index algorithm for monitoring mitigation strategies effects on desertification change in an arid environment. Mitig Adapt Strateg Glob 20(2):263–276

Baret F, Guyot G (1991) Potentials and limits of vegetation indices for LAI and APAR assessment. Remote Sens Environ 35(2):161–173

Beeri O, Phillips R, Hendrickson J, Frank AB, Kronberg S (2007) Estimating forage quantity and quality using aerial hyperspectral imagery for northern mixed-grass prairie. Remote Sens Environ 110:216–225. https://doi.org/10.1016/j.rse.2007.02.027

Berhanu G, Pender J, Ehui SK, Mitiku H (2003) Policies for sustainable land management in the highlands of Tigray, northern Ethiopia: summary of papers and proceedings of a workshop held at Axum Hotel, Mekelle, Ethiopia, 28–29 March 2002. Socio-economics and policy research working paper 54, Kenya

Berk A (2008) Analytically derived conversion of spectral band radiance to brightness temperature. J Quant Spectrosc Radiat Transf 109(7):1266–1276

Bewket W (2007) Soil and water conservation intervention with conventional technologies in northwestern highlands of Ethiopia: acceptance and adoption by farmers. Land Use Policy 24(2):404–416

Bizuneh A (2014) Modeling the effect of climate and land use change on the water resources in northern Ethiopia: The case of Suluh River Basin. Freie Universität Berlin. p 153

Chander G, Markham B, Helder D (2009) Summary of current radiometric calibration coefficients for Landsat MSS, TM, ETM+, and EO-1 ALI sensors. Remote Sens Environ 113:893–903

Carlson TN, Ripley DA (1997) On the relation between NDVI, fractional vegetation cover, and leaf area index. Remote Sens Environ 62(3):241–252

Carlson T, Gillies R, Perry E (1994) A method to make use of thermal infrared temperature and NDVI measurements to infer surface soil water content and fractional vegetation cover. Remote Sens Rev 9(1–2):161–173

Carolyn T, Kwadwo A (2011) Responding to land degradation in the highlands of Tigray, northern Ethiopia, IFPRI discussion paper 01142

Chawla A, Kumar A, Rajkumar S, Singh RD, Thukral AK (2010) Correlation of multispectral satellite data with plant species diversity vis-à-vis soil characteristics in a landscape of Western Himalayan Region, India. Appl Remote Sens 1–1:1–13

Davenport M, Nicholson S (1993) On the relation between rainfall and the normalized difference vegetation index for diverse vegetation types in East Africa. Int J Remote Sens 14(12):2369–2389

Dercon S, Zeitlin A (2009) Rethinking agriculture and growth in Ethiopia: a conceptual discussion. Paper prepared as part of a study on agriculture and growth in Ethiopia. http://www.economics.ox.ac.uk/members/Stefan.Dercon/ethiopiapaper2_v2.pdf. Accessed 6 Apr 2017

EBI (2014) Government of the Federal Democratic Republic of Ethiopia: Ethiopia's fifth national report to the convention on biological diversity Ethiopian. Biodiversity Institute, Addis Ababa

Esser K, Vågen TG, Yibebe T, Mitiku H (2002) Soil and water conservation in Tigray, Ethiopia

Evans J (1996) Straightforward statistics for the behavioral sciences. Brooks/Cole, Boston

FAO (2006) Guidelines for Soil Description, 4th edn. Rome, p 97

Gebremichael D, Nyssen J, Poesen J, Deckers J, Haile M, Govers G, Moeyersons J (2005) Effectiveness of stone bunds in controlling soil erosion on cropland in the Tigray Highlands, northern Ethiopia. Soil Use Manag 21(3):287–297

Gillies R, Carlson T (1995) Thermal remote sensing of surface soil water content with partial vegetation cover for incorporation into climate models. J Appl Meteorol 34:745–756

Gillies R, Kustas W, Humes K (1997) A verification of the 'triangle' method for obtaining surface soil water content and energy fluxes from remote measurements of the normalized difference vegetation. Int J Remote Sens 18(15):3145–3166

Huete AR (1988) A soil-adjusted vegetation index (SAVI). Remote Sens Environ 25:295–309

Kahsai G (2015) Participatory watershed management as the driving force for sustainable livelihood change in the community: the case of Abreha we Atsebeha. In: Nicol A, Langan S, Victor M, Gonsalves J (eds) Water-smart agriculture in East Africa. International Water Management Institute (IWMI), Addis Ababa, p 352. https://doi.org/10.5337/2015.203

Karnieli A, Agam N, Pinker RT, Anderson M, Imhoff ML, Gutman GG, Goldberg A (2010) Use of NDVI and land surface temperature for drought assessment: merits and limitations. J Clim 23(3):618–633

Kassie M, Pender J, Yesuf M, Kohlin G (2008) Estimating returns to soil conservation adoption in the northern Ethiopian highlands. Agric Econ 38(2):213–232

Lambin E, Ehrlich D (1996) The surface temperature-vegetation index space for land cover and land-cover change analysis. Int J Remote Sens 17(3):463–487

Li Z-L, Wu H, Wang N, Qiu S, Sobrino JA, Wan Z, Yan G (2013) Land surface emissivity retrieval from satellite data. Int J Remote Sens 34(9–10):3084–3127. https://doi.org/10.1080/01431161.2012.716540

Moran MS, Clarke TR, Inoue Y, Vidal A (1994) Estimating crop water deficiency using the relation between surface minus air temperature and spectral vegetation index. Remote Sens Environ 49(49):246–263. https://doi.org/10.1016/0034-4257(94)90020-5

NASA (National Aeronautics and Space Administration) (2009) Landsat 7 science data users handbook. http://landsathandbook.gsfc.nasa.gov/handbook/handbook_toc.html. Accessed 13 Dec 17

Negusse T, Yazew E, Tadesse N (2013) Quantification of the impact of integrated soil and water conservation measures on groundwater availability in Mendae Catchment, Abraha We-Atsebaha, eastern Tigray, Ethiopia. Momona Ethiop J Sci 5(2):117–136

Nyssen J, Poesen J, Deckers J (2009) Land degradation and soil and water conservation in tropical highlands. Soil Tillage Res 103(2):197–202

Park KH, Qu ZQ, Wan QQ, Ding GD, Wu B (2013) Effects of enclosures on vegetation recovery and succession in Hulunbeier steppe, China. For Sci Technol 9(1):25–32

Rondeaux G, Steven M, Baret F (1996) Optimization of soil-adjusted vegetation indices. Remote Sens Environ 55:95–107

Rouse JW Jr, Haas RH, Schell JA, Deering DW (1973) Monitoring vegetation system in the great plains with ERTS. Remote sensing center, A&M University, College Station

Sahana M, Ahmed R, Sajjad H (2016) Analyzing land surface temperature distribution in response to land use/land cover change using split window algorithm and spectral radiance model in Sundarban Biosphere Reserve, India. Model Earth Syst Environ 2:81. https://doi.org/10.1007/s40808-016-0135-5

Sahebjalal E, Dashtekian K (2013) Analysis of land use-land covers changes using normalized difference vegetation index (NDVI) differencing and classification methods. Afr J Agric Res 8(37):4614–4622

Sandholt I, Rasmussen K, Andersen J (2002) A simple interpretation of the surface temperature/vegetation index space for assessment of surface moisture status. Remote Sens Environ 79:213–224

Selassie YG, Anemut F, Addisu S, Abera B, Alemayhu A, Belayneh A, Getachew A (2015) The effects of land use types, management practices and slope classes on selected soil physico-chemical properties in Zikre watershed, north-western Ethiopia. Environ Syst Res 4(1):3

Sobrino JA, Raissouni N (2000) Toward remote sensing methods for land cover dynamic monitoring: application to Morocco. Int J Remote Sens 21(2):353–366

Sobrino JA, Jiménez-Muñoz JC, Paolini L (2004) Land surface temperature retrieval from LANDSAT TM 5. Remote Sens Environ 90(4):434–440

Sun Q, Wu Z, Tan J (2012) The relationship between land surface temperature and land use/land cover in Guangzhou, China. Environ Earth Sci 65(6):1687–1694

Suresh S, Ajay SV, Mani K (2016) Estimation of land surface temperature of high range mountain landscape of Devikulam Taluk using Landsat 8 data. Int J Res Eng Technol 5:92–96

Taye G, Poesen J, Wesemael BV, Vanmaercke M, Teka D, Deckers J, Goosseb T, Maetensb W, Nyssen J, Hallet V, Haregeweyn N (2013) Effects of land use, slope gradient, and soil and water conservation structures on runoff and soil loss in semi-arid northern Ethiopia. Phys Geogr 34(3):236–259

Valor E, Caselles V (1996) Mapping land surface emissivity from NDVI: application to European, African, and South American areas. Remote Sens Environ 57(3):167–184

Van der Veen A, Tagel G (2011) Effects of policy intervention on food security in Tigray, northern Ethiopia. Ecol Soc 16(1):18

Weng Q (2009) Thermal infrared remote sensing for urban climate and environmental studies: methods, applications, and trends. ISPRS J Photogramm Remote Sens 64(4):335–344

Weng Q, Lu D, Schubring J (2004) Estimation of land surface temperature-vegetation abundance relationship for urban heat island studies. Remote Sens Environ 89(4):467–483

Whiting A (2017) Ethiopia's Tigray Region bags gold award for greening its drylands. https://www.reuters.com/article/us-land-farming/ethiopias-tigray-region-bags-gold-award-for-greening-its-drylands-idUSKCN1B21CT. Accessed 25 Nov 2017

Yue W, Xu J, Tan W, Xu L (2007) The relationship between land surface temperature and NDVI with remote sensing: application to Shanghai Landsat 7 ETM+ data. Int J Remote Sens 28(15):3205–3226